

Characterization and Reactivity of Copper(II) and Copper(III) σ -Aryl Intermediates in Aminoquinoline-Directed C–H Functionalization

Isaac M. Blythe,^a Jingtong Xu,^b Joaquin S. Fernandez Odell,^b Jeff W. Kampf,^a Miriam A. Bowring,^b and Melanie S. Sanford^{a*}

^aDepartment of Chemistry, University of Michigan, 930 N. University Avenue, Ann Arbor, MI, 48109, United States

^bDepartment of Chemistry, Reed College, 3203 Woodstock Boulevard, Portland, OR, 97202, United States

KEYWORDS organometallics, C–H activation, copper, directing group, KIE

ABSTRACT: Over the past decade, numerous reports have focused on the development and applications of Cu-mediated C–H functionalization reactions; however, to date, little is known about the Cu intermediates involved in these transformations. This Article details the observation and characterization of Cu^{II} and Cu^{III} intermediates in aminoquinoline-directed C(sp²)–H functionalization of a fluoroarene substrate. An initial C(sp²)–H activation at Cu^{II} occurs at room temperature to afford an isolable anionic cyclometalated Cu^{II} complex. This complex undergoes single electron oxidation with ferrocenium or Ag^I salts under mild conditions (5 min at room temperature) to afford C(sp²)–C(sp²) or C(sp²)–NO₂ coupling products. Spectroscopic studies implicate the formation of a transient diamagnetic Cu^{III}- σ -aryl intermediate that undergoes either (i) a second C(sp²)–H activation at Cu^{III} followed by C–C bond-forming reductive elimination or (ii) reaction with an NO₂[–] nucleophile and C(sp²)–NO₂ coupling.

Introduction

Copper salts mediate a wide variety of directed C–H functionalization reactions to form both carbon–carbon and carbon–heteroatom bonds.^{1–3} These transformations are generally proposed to proceed by C–H activation at Cu^{II} to form neutral or anionic cyclometalated Cu^{II} species [A or B in Figure 1, with aminoquinoline (AQ) as a representative directing group] followed by oxidative functionalization via Cu^{III} intermediates of general structure C. However, despite extensive development of these transformations, little is known about the putative organometallic intermediates, including the nature of the supporting ligands (L, X, Nu) under various conditions, the oxidation state of Cu at different stages of the reaction, or the pathway(s) for C–H bond activation. Insights into the structure and reactivity of key intermediates could ultimately inform the rational design of next-generation Cu-mediated C–H functionalization reactions. For instance, in transformations where NuH is a second C–H substrate (e.g., C–H oxidative couplings),^{4–8} a detailed understanding of the two discrete C–H activation steps could guide the expansion of scope and tuning of selectivity.

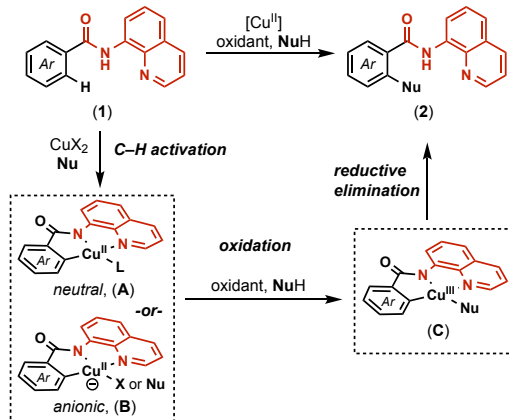


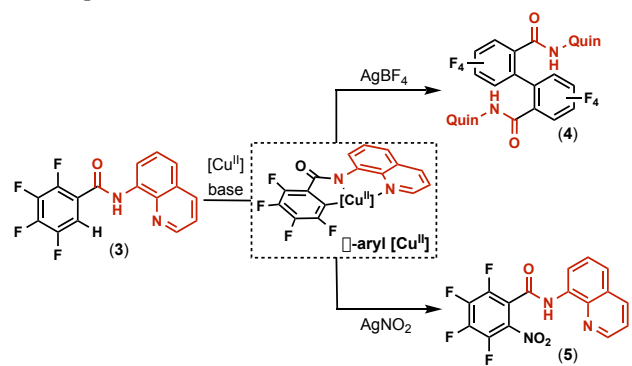
Figure 1. Proposed pathway and organometallic intermediates in Cu-promoted aminoquinoline-directed C–H functionalization.

To date, none of the proposed σ -aryl Cu intermediates (e.g., A–C in Figure 1) in these transformations have proven isolable.⁹ Instead, they have been interrogated computationally or via *in situ* mass spectrometry (MS) experiments. In an example of the former, Stahl and co-workers conducted DFT calculations on a Cu-mediated AQ-directed C(sp²)–H methoxylation reaction.¹⁰ These calculations implicated C(sp²)–H activation at Cu^{II} via a concerted metalation deprotonation (CMD) mechanism to form an anionic Cu^{II} complex bearing methoxide and a cyclometalated AQ ligand (B in Figure 1). The carbon–oxygen coupling step was then proposed to proceed via oxidation to Cu^{III} followed by C–O bond-forming reductive elimination. In a second example, independent studies by Ranu¹¹ and Sun¹² conducted *in situ* MS analysis of Cu-mediated AQ-directed C(sp²)–H

amidation and hydroxylation reactions. Both studies showed *m/z* ratios consistent with the Cu^{III} intermediate **C**. However, we note that **C** is indistinguishable from a Cu^I-product complex by mass.

There are two main challenges for isolating and characterizing these putative organometallic Cu intermediates. First, σ -aryl Cu complexes are often kinetically labile, which hampers efforts to isolate them.^{9a,b,e,14b} Second, the *in situ* monitoring of these transient species by NMR spectroscopy is impeded by the presence of paramagnetic species. We hypothesized that both challenges could be addressed by incorporating fluorine atoms onto the aryl ring of the AQ substrate (**3** in Scheme 1).¹³ Cu complexes bearing fluorinated σ -aryl ligands are known to be much more kinetically stable than their non-fluorinated counterparts.^{14,15} In addition, we hypothesized that the fluorine substituents would serve as ¹⁹F NMR spectroscopic handles, facilitating the monitoring of both diamagnetic and paramagnetic intermediates.¹⁶

We report herein that this fluorination strategy enables the detection and detailed study of σ -aryl Cu intermediates involved in the oxidative dimerization of **3** to form **4** as well as in the oxidative nitration of **3** to form **5** (Scheme 1). Notably, related Cu-mediated oxidative dimerization⁴⁻⁶ and cross-coupling^{7,8} reactions have been widely explored for constructing different types of C–C bonds. Furthermore, several Cu-mediated directed C–H nitration reactions have been disclosed as a route to aromatic C–NO₂ bonds.¹⁷ However, to date, mechanistic details about both classes of reactions remain limited.¹⁸ Our studies reveal that initial C(sp²)–H activation of **3** occurs at Cu^{II} to afford an anionic cupracycle (analogue of **B**, Figure 1) in which a second equivalent of **3** serves as an LX-type (bidentate, neutral-anionic) ligand for the Cu center. Single-electron oxidation of this σ -aryl Cu^{II} complex with weakly nucleophilic oxidants (e.g., ferrocenium tetrafluoroborate (FcBF₄) or AgBF₄) yields oxidative dimerization product **4**. In contrast, with more nucleophilic AgNO₂ as the oxidant, product **5** is formed selectively. Spectroscopic monitoring implicates a Cu^{III} intermediate in both of these transformations. Overall, this study provides some of the first detailed insight into intermediates in aminoquinoline directed C–H activation and oxidative functionalization sequences at Cu centers.

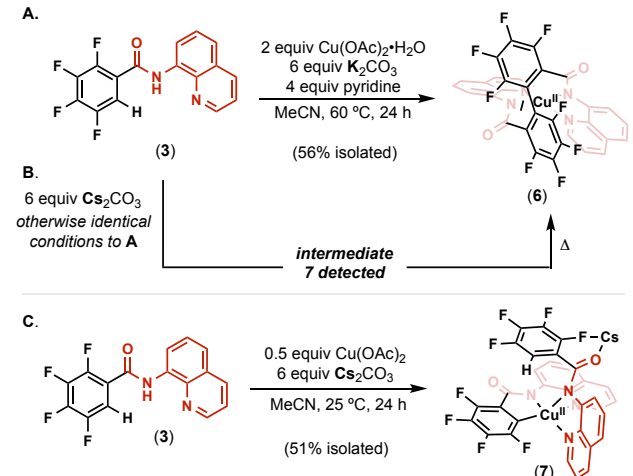


Scheme 1. *This work*: organometallic Cu intermediates in the oxidative functionalization of **3** to form **4** or **5**.

Results and Discussion

Cyclometalation of 3 at Cu(II). We first explored the reaction of **3** with 2 equiv of Cu(OAc)₂·H₂O (a typical mediator for directed C–H functionalization) in the presence of bases that are commonly used in such transformations.¹⁻¹² The addition of 6 equiv K₂CO₃ and 4 equiv of pyridine in MeCN at 60 °C led to

the formation of a single major Cu-containing product (**6**) that was isolated in 56% yield (Scheme 2A). The ¹⁹F NMR spectrum of this paramagnetic Cu^{II} complex shows diagnostic broad resonances between -139 and -156 ppm. Further characterization via EPR, HRMS, elemental analysis, and X-ray crystallography revealed that **6** is a Cu^{II} complex in which the product of C(sp²)–H activation/C–C coupling (**4**) is bound as a tetradentate L₂X₂ ligand (see ORTEP structure in Figure 2A). The excess Cu^{II} (2 equiv relative to **3**) serves as the oxidant for dimerization under these conditions (*vide infra*).¹⁰



Scheme 2. (A) Oxidative dimerization of **3** to form **6**. (B) Intermediate **7** detected upon switching base from K₂CO₃ to Cs₂CO₃. (C) Isolation of cupracycle **7**.

No intermediates were observed by ¹⁹F NMR spectroscopy during the reaction in Scheme 2A. However, changing the base from K₂CO₃ to Cs₂CO₃ under otherwise identical conditions resulted in the formation of a transient species, **7**, characterized by distinctive broad ¹⁹F NMR resonances between -142 and -163 ppm (Scheme 2B). After some optimization, we identified conditions under which **7** is the major product. The most notable changes in reaction conditions were lowering the temperature from 60 to 25 °C and modifying the **3** : Cu ratio from 1 : 2 to 2 : 1. Complex **7** was isolated in 51% yield and characterized by EPR, HRMS, elemental analysis, and X-ray crystallography. These data all show that **7** is an anionic cyclometalated Cu^{II} complex containing a second equivalent of **3** bound as an LX-type ligand. The key role of Cs in the formation of **7** is evident from the X-ray crystal structure (Figure 2B), which shows close contacts between the charge-balancing Cs cation and both the C=O (Cs---O = 2.957 Å) and the ortho fluorine (Cs---F = 3.315 Å) atoms of the LX-type ligand. The formation of **7** is consistent with Stahl and co-workers' DFT calculations implicating an anionic cupracycle in a related reaction.¹⁰ Furthermore, their calculations support a concerted metalation deprotonation (CMD)-type mechanism¹⁹ for aminoquinoline-directed C(sp²)–H activation at Cu^{II} in the presence of carbonate bases under conditions very similar to those in Scheme 2C.²⁰ The C(sp²)–H bond of the fluorinated aryl group in **3** is significantly more acidic than that in the unsubstituted phenyl of Stahl's system, which should further favor a CMD pathway.²¹

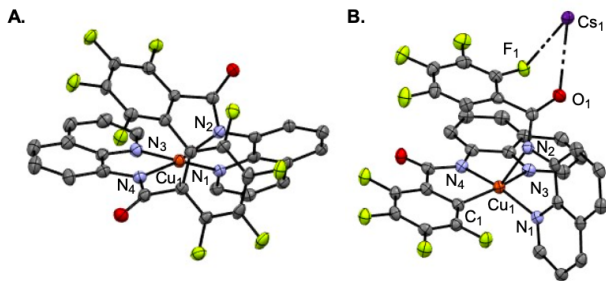


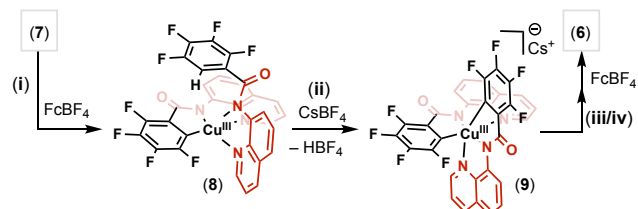
Figure 2. (A) ORTEP diagram for complex **6**. Hydrogen atoms and solvent molecules omitted for clarity; thermal ellipsoids drawn at 50% probability. Bond lengths (Å): Cu₁-N₁ = 1.982, Cu₁-N₂ = 1.957, Cu₁-N₃ = 1.990, Cu₁-N₄ = 1.982; (B) ORTEP diagram for complex **7**. Hydrogen atoms and solvent molecules omitted for clarity; thermal ellipsoids drawn at 50% probability. Bond lengths (Å): Cu₁-N₁ = 2.019, Cu₁-N₂ = 2.245, Cu₁-N₃ = 2.078, Cu₁-N₄ = 1.969, Cu₁-C₁ = 2.002, Cs₁-O₁ = 2.957, Cs₁-F₁ = 3.315.

Reaction of 7 with non-nucleophilic oxidants. We next focused on establishing the pathway from cyclometalated Cu^{II} complex **7** to the C–C coupled product **6**. To initially probe for the accessibility of high valent Cu, cyclic voltammetry (CV) studies were conducted in MeCN/NBu₄PF₆. At a scan rate of 100 mV/s, the CV of **7** shows a quasi-reversible single-electron oxidation at -0.11 V vs Ag/Ag⁺ (see Supporting Information), consistent with a Cu^{II/III} couple. Based on this result, the chemical oxidation of **7** was conducted using oxidants with potentials close to 0 V [ferrocenium tetrafluoroborate (FcBF₄) or AgBF₄]. As shown in Table 1, treatment with these oxidants resulted in the near quantitative conversion of **7** to **6** within 5 min at room temperature (entries 1 and 2). The expected oxidant under the conditions in Scheme 2A is the Cu^{II} pyridine (py) complex Cu₂(OAc)₄(py)₂,¹⁰ and this also reacts with **7** to form **6** in 97% yield at 60 °C in 24 h (entry 3).

entry	oxidant	conditions	yield 6 (%)	2 equiv oxidant
				conditions
1	FcBF ₄	25 °C, <5 min	90	
2	AgBF ₄	25 °C, <5 min	97	
3	Cu ₂ (OAc) ₄ (py) ₂	60 °C, 24 h	97	

Table 1. Oxidatively-induced conversion of **7** to **6**. Yields determined by ¹⁹F NMR spectroscopy based on an internal standard.

Overall, the results in Table 1 indicate that the conversion of **7** to **6** is triggered by the oxidation of Cu^{II} to Cu^{III}. A potential pathway for this transformation is outlined in Scheme 3 and involves (i) oxidation of **7** to the neutral Cu^{III} intermediate **8**, (ii) C(sp²)-H activation of the pendant aryl group at Cu^{III} to generate the 6-coordinate anionic bis-σ-aryl intermediate **9**,²² and (iii/iv) C(sp²)-C(sp²) bond-forming reductive elimination followed by single electron oxidation to afford **6**.



Scheme 3. Possible pathway for the oxidatively-induced conversion of **7** to **6**. Steps: (i) oxidation of Cu^{II} to Cu^{III}, (ii) C(sp²)-H activation at Cu^{III}, and (iii/iv) reductive elimination/1e⁻ oxidation.

Detecting intermediates in conversion of 7 to 6. In an effort to detect the putative Cu^{III} intermediates **8** and **9**, we monitored the FcBF₄-promoted conversion of **7** to **6** via UV-vis spectroscopy. The treatment of a 75 μM MeCN solution of **7** ($\lambda_{\text{max}} = 386$ nm) with FcBF₄ at room temperature resulted in rapid and quantitative formation of an intermediate (**I**) with $\lambda_{\text{max}} = 349$ nm (Figure 3). The hypsochromic shift is consistent with formulation of **I** as a Cu^{III} species.²³ The compound decays over 30 min at room temperature to afford **6** ($\lambda_{\text{max}} = 373$ nm).

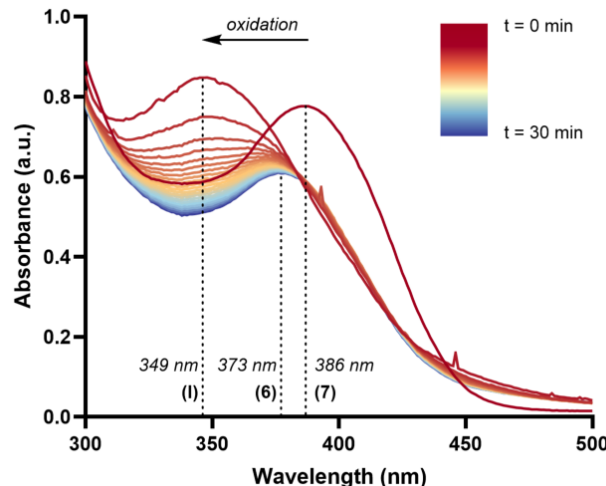
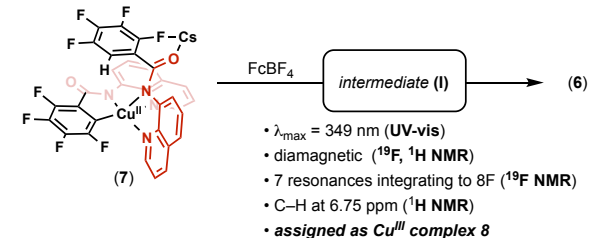
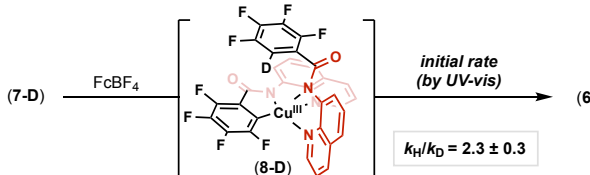


Figure 3. Monitoring the reaction of **7** with FcBF₄ via UV-vis spectroscopy (75 μM [7] in MeCN at room temperature) (shown) and NMR spectroscopy (9.6 mM [7] in MeCN at -15 °C).

Extensive efforts to isolate **I** by recrystallization at low temperature were unsuccessful. As such, **I** was also characterized *in situ* by NMR spectroscopy. Cold (-15 °C) solutions of **7** and FcBF₄ in acetonitrile were combined in an NMR tube, and this mixture was inserted into an NMR probe pre-cooled to -15 °C. Analysis by ¹⁹F NMR spectroscopy showed the formation of an intermediate (**I**) with 7 distinct ¹⁹F NMR resonances (integrating to 8 total fluorine atoms) between -130 and -158 ppm. The presence of two unique fluoroaryl groups indicates that **I** is not **9** (in which the fluoroaryl groups are equivalent). ¹H NMR spectroscopic analysis revealed that **I** is diamagnetic, as indicated by the appearance of aromatic resonances between 6.5 and 9.5 ppm. These signals integrate to 13 hydrogen atoms indicating that the C(sp²)-H bond remains intact in **I**. Finally, warming the NMR solutions of **I** to 25 °C resulted in clean conversion to **6** as determined by ¹⁹F NMR spectroscopy.

Overall, these data are consistent with the formulation of **I** as Cu^{III} complex **8**, the initial product of one-electron oxidation of

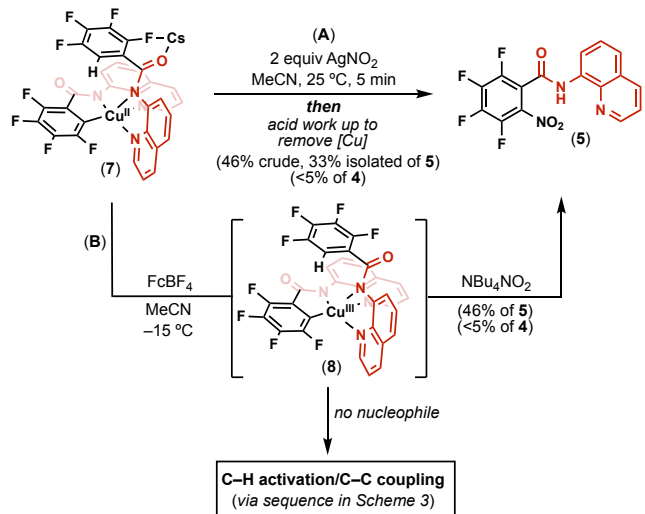
7. To further support this assignment, as well as to interrogate the pathway from **8** to **6**, we synthesized **8-D**, in which the fluoroaryl hydrogen is deuterated.²⁴ If C–H activation occurs at or before the rate determining step in the conversion of **8** to **6**, we would expect to see a 1° kinetic isotope effect. UV-vis spectroscopy was employed to obtain initial rates for the decay of **8** and **8-D** (generated *in situ* by the treatment of **7** and **7-D** with FcBF_4). The observed isotope effect ($k_{\text{H}}/k_{\text{D}} = 2.3 \pm 0.3$; Scheme 4) supports the mechanism shown in Scheme 3 in which $\text{C}(\text{sp}^2)$ –H activation occurs at Cu^{III} complex **8** and is the rate determining step in the conversion of **8** to **6**.



Scheme 4. Isotope effect for conversion of **8/8-D** to **6**.

This isotope effect is comparable to that reported for a related intramolecular $\text{C}(\text{sp}^2)$ –H cleavage at Ni^{IV} (where $k_{\text{H}}/k_{\text{D}} \sim 3$).^{22e} In the Ni^{IV} system, DFT studies implicated a $\text{S}_{\text{E}}\text{Ar}$ pathway at the highly electrophilic Ni^{IV} center, with the proton released as triflic acid. We propose that a similar pathway is likely in this system, generating HBF_4 along with **9**.

Carbon-heteroatom coupling at 7. Finally, we sought to evaluate whether oxidatively-induced $\text{C}(\text{sp}^2)$ –heteroatom coupling can occur from **7** with an oxidant bearing a more nucleophilic counterion. As discussed above, the use of AgBF_4 results in selective $\text{C}(\text{sp}^2)$ – $\text{C}(\text{sp}^2)$ coupling. We noted literature reports that employed AgNO_2 to achieve Cu-mediated aminoquinoline-directed $\text{C}(\text{sp}^2)$ –H nitration and thus hypothesized that this Ag^{I} oxidant/nucleophile might promote the nitration of **7**.¹⁷ Indeed, the treatment of **7** with 2 equiv of AgNO_2 at room temperature (Scheme 5A) resulted in an instantaneous color change from dark red to brown along with the formation of a precipitate (presumably Ag^0). Analysis of the crude reaction mixture by ^{19}F and ^1H NMR spectroscopy (following an acidic workup to remove the Cu) showed the formation of the $\text{C}(\text{sp}^2)$ – NO_2 coupling product **5** in 46% yield. Product **5** was isolated in 33% yield, and its identity was confirmed by NMR spectroscopy and HRMS to match that of an independently synthesized authentic sample (see SI for details). Notably, <5% of the C–C coupling product **4** was detected, indicating that $\text{C}(\text{sp}^2)$ – NO_2 coupling is faster than C–H activation/C–C coupling with this oxidant.



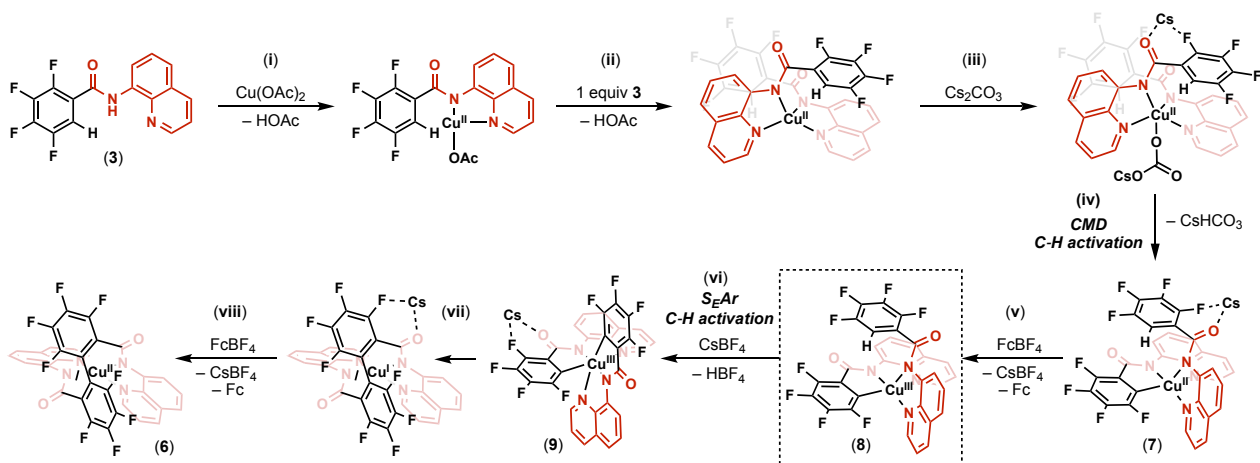
Scheme 5. $\text{C}(\text{sp}^2)$ – NO_2 coupling from **7** with (A) AgNO_2 ; (B) FcBF_4 followed by NBu_4NO_2

In a first attempt to detect Cu intermediates for the nitration reaction, the reaction of **7** with AgNO_2 was monitored by ^{19}F NMR spectroscopy at -15°C . However, due to the formation of a large amount of precipitate, the resonances were broad and difficult to assign (see p. S37). We next explored the sequential oxidation of **7** with FcBF_4 at -15°C (to form Cu^{III} complex **8** *in situ*) followed by the addition of 2 equiv of NBu_4NO_2 (Scheme 5B). Again, this reaction was difficult to analyze by ^{19}F NMR spectroscopy due to the formation of a large amount of precipitate upon the addition of NBu_4NO_2 . However, after acidic workup, nitrated product **5** was observed in 46% yield, along with <5% of the C–C coupled product **4**. This result provides support for a pathway involving $\text{C}(\text{sp}^2)$ – NO_2 coupling from a Cu^{III} intermediate related to (or derived from) **8**.

Summary and Conclusions

In summary, this study describes the detection and isolation of several key intermediates in the aminoquinoline-directed Cu-mediated $\text{C}(\text{sp}^2)$ –H functionalization of a fluoroaryl substrate, **3**. Plausible mechanistic pathways for the formation of the C–C and C–N coupled products are provided in Scheme 6 as well as Schemes S1 and S2, and key implications from this work are outlined below. First, we demonstrate that aminoquinoline-directed $\text{C}(\text{sp}^2)$ –H activation of this fluoroaryl substrate proceeds at Cu^{II} under mild conditions (within 24 h at 25°C). Using a stoichiometry of 2 equiv of substrate **3** to 1 equiv of $\text{Cu}(\text{OAc})_2$ leads to the formation of cyclocuprated product **7**, an anionic Cu^{II} complex containing one cyclometalated (CNN' bound) and one non-cyclometalated (NN') bound aminoquinoline. This type of structure bearing two substrate molecules in different binding modes is not commonly proposed in Cu-mediated $\text{C}(\text{sp}^2)$ –H functionalization reactions; however, we believe that it is likely relevant to many of these transformations, particularly when the substrate is in excess relative to Cu.

A Cs^+ counterion appears to play a crucial role in stabilizing this anionic σ -aryl Cu^{II} species, while the carbonate is important for the CMD C–H activation step.¹⁰ Cs^+ and carbonate salts are used in a variety of other Cu-mediated C–H functionalization reactions and may play a similar role in these systems.^{4,25} We conclude that the identity of the alkali metal counterion for base additives should be considered as a key



Scheme 6. Plausible overall mechanism for the conversion of **6** to **3** involving two different C–H activation steps. Proposed sequence involves: (i) coordination of 1 equiv of **3** to $\text{Cu}(\text{OAc})_2$ with loss of HOAc , (ii) coordination of a second equiv of **3** with loss of HOAc , (iii) coordination of Cs_2CO_3 , (iv) C–H activation via a CMD mechanism to form **7** and CsHCO_3 , (v) single-electron oxidation to afford **8**, (vi) C–H activation at Cu^{III} via an S_{Ar} mechanism to form **9**, (vii) $\text{C}(\text{sp}^2)\text{–C}(\text{sp}^2)$ bond-forming reductive elimination to form a $\text{Cu}(\text{I})$ complex, and (viii) single-electron oxidation of $\text{Cu}(\text{I})$ to generate $\text{Cu}(\text{II})$ product **6**. Intermediate **8** can also react competitively with NBu_4NO_2 as outlined in Schemes 5 and S2.

variable for reaction optimization in Cu-mediated C–H functionalizations.

Finally, we show that cupracycle **7** reacts with ferrocenium tetrafluoroborate (FcBF_4) to form a transient Cu^{III} intermediate (**8**). This intermediate can undergo at least two possible functionalization reactions. In the absence of a nucleophile, a second intramolecular $\text{C}(\text{sp}^2)\text{–H}$ activation can occur at Cu^{III} . This is followed by $\text{C}(\text{sp}^2)\text{–C}(\text{sp}^2)$ coupling to form the product of oxidative dimerization (**6**) (Scheme 6). However, in the presence of nitrite (NO_2^-), $\text{C}(\text{sp}^2)\text{–NO}_2$ coupling occurs to form the nitroarene product **5** (Scheme 5, Scheme S2). A key implication is that product selectivity is dictated by the relative rates of these competing processes at Cu^{III} .

Ongoing studies are focused on studying these relative rates with a wider variety of nucleophiles as well as on evaluating the relevance of intermediates like **7** and **8** in reactions involving less fluorinated substrates. Overall, we anticipate that these mechanistic insights will inform the development of a next generation of Cu-mediated C–H functionalization reactions and serve as a platform for continued mechanistic elucidation.

ASSOCIATED CONTENT

The Supporting Information is available free of charge on the ACS Publications website.

Experimental/methods, spectroscopic and characterization data (PDF)

X-ray crystallographic data for **6** and **7**

Deposition No: 2235935 for **6**; 2235936 for **7**

AUTHOR INFORMATION

Corresponding Author

* Melanie Sanford; Department of Chemistry, University of Michigan, Ann Arbor, MI, 48109, United States; orcid.org/0000-0001-9342-9436; Email: mssanfor@umich.edu

ACKNOWLEDGMENT

We gratefully acknowledge the US National Science Foundation (CHE-1954985) for support. JX was supported by a fellowship from the Paul K. Richter & Evalyn Elizabeth Cook Richter Memorial Fund. JFO was supported by a fellowship from the Alfred W. Weitkamp Student Research Bursary Fund. We also thank Dr. Liam Sharninghausen, Dr. Eugenio Alvarado, and Dr. Irving Rettig for helpful discussions.

REFERENCES

¹ For the first example of AQ-directed C–H functionalization, see: Zaitsev, V. G.; Shabashov, D.; Daugulis, O. *J. Am. Chem. Soc.* **2005**, 127, 13154–13155.

² (a) Gandeepan, P.; Müller, T.; Zell, D.; Cera, G.; Warratz, S.; Ackermann, L. 3d Transition Metals for C–H Activation. *Chem. Rev.* **2019**, 119, 2192–2452. (b) Liu, J.; Chen, G.; Tan, Z. Copper-Catalyzed or -Mediated C–H Bond Functionalizations Assisted by Bidentate Directing Groups. *Adv. Synth. Catal.* **2016**, 358, 1174–1194. (c) Rao, W-H.; Shi, B-F. Recent Advances in Copper-Mediated Chelation-Assisted Functionalization of Unactivated C–H Bonds. *Org. Chem. Front.* **2016**, 3, 1028–1047.

³ (a) Takamatsu, K.; Hirano, K.; Miura, M. Copper-Mediated Decarboxylative Coupling of Benzamides with *ortho*-Nitrobenzoic Acids by Directed C–H Cleavage. *Angew. Chem. Int. Ed.* **2017**, 56, 5353–5357. (b) Mandal, A.; Sahoo, H.; Baidya, M. Copper-Catalyzed 8-Aminoquinoline-Directed Selenylation of Arene and Heteroarene C–H Bonds. *Org. Lett.* **2016**, 18, 3202–3205. (c) Liu, J.; Yu, L.; Zhuang, S.; Gui, Q.; Chen, X.; Wang, W.; Tan, Z. Copper-mediated *ortho* C–H Sulfonylation of Benzoic Acid Derivatives with Sodium Sulfinate. *Chem. Commun.* **2015**, 51, 6418–6421. (d) Zhang, J.; Li, D.; Chen, H.; Wang, B.; Liu, Z.; Zhang, Y. Copper(II)/Silver(I)-Catalyzed Sequential Alkynylation and Annulation of Aliphatic Amides with Alkynyl Carboxylic Acids: Efficient Synthesis of Pyrrolidones. *Adv. Synth. Catal.* **2015**, 358, 792–807. (e) Miura, W.; Hirano, K.; Miura, M. Copper-Mediated Oxidative Coupling of Benzamides with Maleimides via Directed C–H Cleavage. *Org. Lett.* **2015**, 17, 4034–4037. (f) Dong, J.; Wang, F.; You, J. Copper-Mediated Tandem Oxidative $\text{C}(\text{sp}^2)\text{–H/C}(\text{sp})\text{–H}$ Alkynylation and Annulation of Arenes with Terminal Alkynes. *Org. Lett.* **2014**, 16, 2884–2887. (g) Wang, S.; Guo, R.; Wang, G.; Chen, S-Y.; Yu, X-Q. Copper-Catalyzed Phosphorylation of sp^2 C–H Bonds. *Chem. Commun.* **2014**, 50, 12718–12721. (h) Tran, L.; Roane, J.; Daugulis, O. Directed Amination of Non-Acidic Arene C–H Bonds by a Copper–Silver

Catalytic System. *Angew. Chem. Int. Ed.* **2013**, *52*, 6043-6046. (i) Roane, J.; Daugulis, O. Copper-Catalyzed Etherification of Arene C–H Bonds. *Org. Lett.* **2013**, *15*, 5842-5845. (j) Tran, L.; Popov, I.; Daugulis, O. Copper-Promoted Sulfonylation of sp^2 C–H Bonds. *J. Am. Chem. Soc.* **2012**, *134*, 18237-18240.

⁴ Odani, R.; Nishino, M.; Hirano, K.; Satoh, T.; Miura, M. Copper-Mediated Regioselective Homocoupling of Thiophenes and Indoles via Directed C–H Cleavage. *Heterocycles* **2014**, *88*, 595-602.

⁵ Le, J.; Gao, Y.; Ding, Y.; Jiang, C. Cu-Mediated C2-Dehydrogenative Homocoupling of Indoles via C–H Activation Assisted by a Removable *N*-Pyrimidyl Directing Group. *Tetrahedron Lett.* **2016**, *57*, 1728-1731.

⁶ Singh, B.; Jana, R. Ligand Enabled, Copper-Promoted Regio- and Chemoselective Hydroxylation of Arenes, Aryl Halides, and Aryl Methyl Esters. *J. Org. Chem.* **2016**, *81*, 831-841.

⁷ For examples of directed Cu-mediated C–H oxidative cross-coupling, see: (a) Kajiwara, R.; Xu, S.; Hirano, K.; Miura, M. Bipyridine-Type Bidentate Auxiliary-Enabled Copper-Mediated C–H/C–H Biaryl Coupling of Phenols and 1,3-Azoles. *Org. Lett.* **2021**, *23*, 5405-5409. (b) Tan, G.; Zhang, L.; Liao, X.; Shi, Y.; Wu, Y.; Yang, Y.; You, J. Copper- or Nickel-Enabled Oxidative Cross-Coupling of Unreactive C(sp³)–H Bonds with Azole C(sp²)–H Bonds: Rapid Access to β -Azoyl Propanoic Acid Derivatives. *Org. Lett.* **2017**, *19*, 4830-4833. (c) Wu, X.; Zhao, Y.; Ge, H. Pyridine-Enabled Copper-Promoted Cross Dehydrogenative Coupling of C(sp²)–H and Unactivated C(sp³)–H Bonds. *Chem. Sci.* **2015**, *6*, 5978-5983. (d) Zhao, S.; Yuan, J.; Li, Y.-C.; Shi, B.-F. Copper-Catalyzed Oxidative C–H/C–H Cross-Coupling of Benzamides and Thiophenes. *Chem. Commun.* **2015**, *51*, 12823-12826. (e) Odani, R.; Hirano, K.; Satoh, T.; Miura, M. Copper-Mediated C6-Selective Dehydrogenative Heteroarylation of 2-Pyridones with 1,3-Azoles. *Angew. Chem. Int. Ed.* **2014**, *53*, 10784-10788.

⁸ Reviews on oxidative C–H coupling: (a) Bansal, S.; Shabade, A.; Punji, B. Advances in C(sp²)–H/C(sp²)–H Oxidative Coupling of (Hetero)arenes Using 3d Transition Metal Catalysts. *Adv. Synth. Catal.* **2021**, *363*, 1998-2022. (b) Yan, Y. D.; Lan, J. B.; You, J. S. Oxidative C–H/C–H Coupling Reactions between Two (Hetero)arenes. *Chem Rev.* **2017**, *117*, 8787-8863. (c) Maheswari, C. U.; Kumar, G. S.; Reddy, K. R. Recent Advances in Copper-Catalyzed Oxidative Cross-Coupling Chemistry. *Curr. Org. Chem.* **2016**, *20*, 512-579. (d) Dong, J.; Wu, Q.; You, J. Stoichiometric Copper or Silver Salt-Mediated Oxidative C–H/C–H Cross-Coupling Reactions. *Tetrahedron Lett.* **2015**, *56*, 1591-1599.

⁹ For examples of the isolation of σ -aryl Cu^{II} and Cu^{III} complexes bearing macrocyclic ligands, see: (a) Ribas, X.; Devillard, M. Model Macrocyclic Ligands for Proof-of-Concept Mechanistic Studies in Transition-Metal Catalysis. *Chem. Eur. J.* **2017**, *24*, 1222-1230. (b) Casitas, A.; Ribas, X. The Role of Organometallic Copper(III) Complexes in Homogeneous Catalysis. *Chem. Sci.* **2013**, *4*, 2301-2318. (c) Yao, B.; Wang, D.-X.; Huang, Z.-T.; Wang, M.-X. Room-Temperature Aerobic Formation of a Stable Aryl-Cu(III) Complex and its Reactions with Nucleophiles: Highly Efficient and Diverse Arene C–H Functionalizations of Azacalic[1]arene[3]pyridine. *Chem. Commun.* **2009**, *20*, 2899-2901. (d) Maeda, H.; Osuka, A.; Ishikawa, Y.; Aritome, I.; Hisaeda, Y.; Furuta, H. N-Confused Porphyrin-Bearing *meso*-Perfluorophenyl Groups: A Potential Agent That Forms Stable Square-Planar Complexes with Cu(II) and Ag(III). *Org. Lett.* **2003**, *5*, 1293-1296. (e) Ribas, X.; Jackson, D.; Donnadieu, B.; Mahía, J.; Parella, T.; Xifra, R.; Hedman, B.; Hodgson, K.; Llobet, A.; Stack, D. Aryl C–H Activation by Cu^{II} to Form an Organometallic Aryl–Cu^{III} Species: A Novel Twist on Copper Disproportionation. *Angew. Chem. Int. Ed.* **2002**, *41*, 2991-2994. (f) Chmielewski, P.; Łatos-Grażyński, L.; Schmidt, I. Copper(II) Complexes of Inverted Porphyrin and Its Methylated Derivatives. *Inorg. Chem.* **2000**, *39*, 5475-5482.

¹⁰ Suess, A.; Ertem, M.; Cramer, C.; Stahl, S. Divergence between Organometallic and Single-Electron-Transfer Mechanisms in Copper(II)-Mediated Aerobic C–H Oxidation. *J. Am. Chem. Soc.* **2013**, *135*, 26, 9797-9804.

¹¹ Ghosh, T.; Maity, P.; Ranu, B. Cu(OAc)₂-Promoted Ortho C(sp)²–H Amidation of 8-Aminoquinoline Benzamide with Acyl Azide:

Selective Formation of Aroyl or Acetyl Amide Based on Catalyst Loading. *J. Org. Chem.* **2018**, *83*, 11758-11767.

¹² Wang, M.; Hu, Y.; Jiang, Z.; Shen, H.; Sun, X. Divergent Copper-Mediated Dimerization and Hydroxylation of Benzamides Involving C–H bond Functionalization. *Org. Biomol. Chem.* **2016**, *14*, 4239-4246.

¹³ (a) Furuta, H.; Maeda, H.; Osuka, A. Doubly N-Confused Porphyrin: A New Complexing Agent Capable of Stabilizing Higher Oxidation States. *J. Am. Chem. Soc.* **2000**, *122*, 803-807. (b) Satterlee, J. Fundamental Concepts of NMR in Paramagnetic Systems. Part II: Relaxation Effects. *Concepts Magn. Reson.* **1990**, *2*, 119-129.

¹⁴ (a) Wang, G.; Li, M.; Leng, X.; Xue, X.; Shen, Q. Neutral Five-Coordinate Arylated Copper(III) Complex: Key Intermediate in Copper-Mediated Arene Trifluoromethylation. *Chin. J. Chem.* **2022**, *40*, 1924-1930. (b) Kundu, S.; Greene, C.; Williams, K.; Salvador, T.; Bertke, J.; Cundari, T.; Warren, T. Three-Coordinate Copper(II) Aryls: Key Intermediates in C–O Bond Formation. *J. Am. Chem. Soc.* **2017**, *139*, 9112-9115. (c) Molteni, R.; Edkins, K.; Haehnel, M.; Steffen, A. C–H Activation of Fluoroarenes: Synthesis, Structure, and Luminescence Properties of Copper(I) and Gold(I) Complexes Bearing 2-Phenylpyridine Ligands. *Organometallics* **2016**, *35*, 629-640.

¹⁵ (a) Milbauer, M.; Kampf, J. F.; Sanford, M. S. Nickel(IV) Intermediates in Aminoquinoline-Directed C(sp²)–C(sp³) Coupling. *J. Am. Chem. Soc.* **2022**, *144*, 21030-21034. (b) Roy, P.; Bour, J. R.; Kampf, J. W.; Sanford, M. S. Catalytically Relevant Intermediates in the Ni-Catalyzed C(sp²)–H and C(sp³)–H Functionalization of Aminoquinoline Substrates. *J. Am. Chem. Soc.* **2019**, *141*, 17382-17387.

¹⁶ Since the fluorines will be relatively remote from the Cu center, we anticipated that their ¹⁹F NMR signals would not be subject to severe paramagnetic broadening.

¹⁷ (a) Katayev, D.; Pfister, K.; Wendling, T.; Gooßen, L. Copper-Mediated *ortho*-Nitration of (Hetero)Arenecarboxylates. *Chem. Eur. J.* **2014**, *20*, 9902-9905. (b) Liu, J.; Zhuang, S.; Gui, Q.; Chen, X.; Yang, Z.; Tan, Z. Copper-Mediated *ortho*-Nitration of Arene and Heteroarene C–H Bonds Assisted by an 8-Aminoquinoline Directing Group. *Adv. Synth. Catal.* **2015**, *357*, 732-738. (c) Wang, C.-M.; Tang, K.-X.; Gao, T.-H.; Chen, L.; Sun, L.-P. Cu(II)-Catalyzed *ortho*-C–H Nitration of Aryl Ureas By C–H Functionalization. *J. Org. Chem.* **2018**, *83*, 8315-8321. (d) Tu, D.; Luo, J.; Chao, J. Copper-Mediated Domino C–H Iodination and Nitration of Indoles. *Chem. Commun.* **2018**, *54*, 2514-2517. (e) Song, L.-R.; Fan, Z.; Zhang, A. Recent Advances in Transition Metal-Catalyzed C(sp²)–H Nitration. *Org. Biomol. Chem.* **2019**, *17*, 1351-1361.

¹⁸ The majority of reported Cu-mediated C–H oxidative couplings and C–H nitration reactions are stoichiometric in Cu(II) [refs. 4-8, 17]. Consistent with this precedent, our attempts to render the reactions in Scheme 1 catalytic in Cu have thus far proven unsuccessful.

¹⁹ (a) Ackermann, L. Carboxylate-Assisted Transition-Metal-Catalyzed C–H Bond Functionalizations: Mechanism and Scope. *2011*, *111*, 1315-1345. (b) Lapointe, D.; Fagnou, K. Overview of the Mechanistic Work on the Concerted Metallation-Deprotonation Pathway. *Chem. Lett.* **2010**, *39*, 1118-1126. (c) Gorelsky, S.; Lapointe, D.; Fagnou, K. Analysis of the Concerted Metallation-Deprotonation Mechanism in Palladium-Catalyzed Direct Arylation Across a Broad Range of Aromatic Substrates. *J. Am. Chem. Soc.* **2008**, *130*, 10848-10849.

²⁰ (a) Kong, F.; Chem, S.; Chen, J.; Liu, C.; Zhu, W.; Dickie, D.; Schinski, W.; Zhang, S.; Ess, D.; Gunnoe, T.B. Cu(II) Carboxylate Arene C–H Functionalization: Tuning for Nonradical Pathways. *Sci. Adv.* **2022**, *8*, eadd1594. (b) Xu, L.-P.; Haines, B.; Ajitha, M.; Yu, J.-Q.; Musaev, D. Unified Mechanistic Concept of the Copper-Catalyzed and Amide-Oxazoline-Directed C(sp²)–H Bond Functionalization. *ACS Catal.* **2021**, *11*, 12620-12631. (c) Kim, H.; Heo, J.; Kim, J.; Baik, M.-H.; Chang, S. Copper-Mediated Amination of Aryl C–H Bonds with the Direct Use of Aqueous Ammonia via a Disproportionation Pathway. *J. Am. Chem. Soc.* **2018**, *140*, 14350-14356. (d) Tang, S.; Gong, T.; Fu, Y. Mechanistic Study of Copper-Catalyzed Intramolecular *ortho*-C–H Activation/Carbon-Nitrogen and Carbon-Oxygen Cyclizations. *Sci. China Chem.* **2013**, *56*, 619-632.

²¹ Lafrance, M.; Rowley, C.; Woo, T.; Fagnou, K. Catalytic Intermolecular Direct Arylation of Perfluorobenzenes. *J. Am. Chem. Soc.* **2006**, *128*, 8754-8756.

²² For examples of related C–H activation reactions at high valent Cu, Ni, and Pd centers, see: (a) Hintz, H.; Bower, J.; Tang, J.; LaLama, M.; Sevov, C.; Zhang, S. Copper-Catalyzed Electrochemical C–H Fluorination. *Chem. Catal.* **2023**, *3*, 100491-100491. (b) Zhang, Q.; Tong, S.; Wang, M-X. Unraveling the Chemistry of High Valent Aryl-copper Compounds and Their Roles in Copper-Catalyzed Arene C–H Bond Transformations Using Synthetic Macrocycles. *Acc. Chem. Res.* **2022**, *55*, 2796-2810. (c) Roberts, C. C.; Chong, E.; Kampf, J. W.; Carty, A. J.; Ariaford, A.; Sanford, M. S. Nickel(II/IV) Manifold Enables Room Temperature C(sp³)–H Functionalization. *J. Am. Chem. Soc.* **2019**, *141*, 19513-19520. (d) Mandal, M.; Elwell, C.; Bouchey, C.; Zerk, T.; Tolman, W.; Cramer, C. Mechanisms for Hydrogen-Atom Abstraction by Mononuclear Copper(III) Cores: Hydrogen-Atom Transfer or Concerted Proton-Coupled Electron Transfer. *J. Am. Chem. Soc.* **2019**, *141*, 17236-17244. (e) Chong, E.; Kampf, J. W.; Ariaford, A.; Carty, A. J.; Sanford, M. S. Oxidatively Induced C–H Activation at High Valent Nickel. *J. Am. Chem. Soc.* **2017**, *139*, 6058-6061. (f) Zhou, W.; Zheng, S.; Schultz, J. W.; Rath, N. P.; Mirica, L. M. Aromatic Cyanoalkylation through Double C–H Activation Mediated by Ni(III). *J. Am. Chem. Soc.* **2016**, *138*, 5777-5780. (g) Maleckis, A.; Kampf, J. W.; Sanford, M. S. Acetate-Assisted C–H Activation at Cationic Palladium(IV) Centers. *J. Am. Chem. Soc.* **2013**, *135*, 6618-6625.

(h) Racowski, J. M.; Ball, N. D.; Sanford, M. S. C–H Bond Activation at Palladium(IV) Centers. *J. Am. Chem. Soc.* **2011**, *133*, 18022-18025.

²³ (a) Figgis, B.; Hitchman, M. *Ligand Field Theory and Its Applications*; Wiley-VCH, 2000; pp 179-227. (b) Wang reports that crystals of a related Cu^{II}/Cu^{III} pair of σ -aryl complexes are red and purple, respectively, consistent with a hypsochromic shift like that seen in our system. See ref. 3b and Zhang, H.; Yao, B.; Zhao, L.; Wang, D-X.; Xu, B-Q.; Wang, M-X. Direct Synthesis of High-Valent Aryl–Cu(II) and Aryl–Cu(III) Compounds: Mechanistic Insight into Arene C–H Bond Metalation. *J. Am. Chem. Soc.* **2014**, *136*, 6326-6332.

²⁴ **8-D** shows aromatic resonances integrating to 12H versus ferrocene. The signal at 6.75 ppm is no longer present, consistent with its assignment as the C(sp²)–H bond on the fluoroaryl ring.

²⁵ (a) Hu, L.; Chen, X.; Gui, Q.; Tan, Z.; Zhu, G. Highly Mono-selective *ortho*-Trifluoromethylation of Benzamides via 8-Aminoquinoline Assisted Cu-Promoted C–H Activations. *Chem. Commun.* **2016**, *52*, 6845-6848. (b) Zhang, Y.; Wang, Q.; Yu, H.; Huang, Y. Directed Arene/Alkyne Annulation Reactions via Aerobic Copper Catalysis. *Org. Biomol. Chem.* **2014**, *12*, 8844-8850.

TOC Figure

